

## Phase Relations of $\text{TlClO}_4$ and $\text{TlBF}_4$ to High Pressures

J. B. CLARK AND CARL W. F. T. PISTORIUS

*National Physical Research Laboratory, South African Council for Scientific and Industrial Research, P.O. Box 395, Pretoria, South Africa*

Received August 30, 1972

Orthorhombic  $\text{TlBF}_4$  III transforms at 201.7°C to cubic  $\text{TlBF}_4$  II, and at 26.6°C,  $6.73 \pm 0.60$  kbar to a high-pressure phase  $\text{TlBF}_4$  IV similar to Bridgman's high-pressure form of  $\text{TlClO}_4$ . The high-pressure phase diagrams of  $\text{TlClO}_4$  and  $\text{TlBF}_4$  were studied by means of differential thermal analysis and volumetric techniques, and found to be closely similar to those of  $\text{RbClO}_4$  and  $\text{RbBF}_4$ .

### Introduction

Bridgman (1) studied the polymorphism of the univalent perchlorates to 50 kbar and ~100°C. More recently the complete phase diagrams to 40 kbar of  $\text{NaBF}_4$ ,  $\text{NaClO}_4$  (2),  $\text{KClO}_4$ ,  $\text{KBF}_4$  (3),  $\text{RbClO}_4$ ,  $\text{RbBF}_4$  (4),  $\text{CsClO}_4$ ,  $\text{CsBF}_4$  (5),  $\text{NH}_4\text{ClO}_4$  and  $\text{NH}_4\text{BF}_4$  (6) have been reported.

The ambient modifications  $\text{TlClO}_4$  II and  $\text{TlBF}_4$  III have the barite structure (7, 8), and are therefore isostructural with the ambient forms of the corresponding potassium, ammonium, rubidium and cesium (9) salts as well as with the high-pressure phases  $\text{NaClO}_4$  III and  $\text{NaBF}_4$  IV (2). These substances all have disordered cubic high-temperature forms (9) with the space group  $Fm\bar{3}m$  (2). This transition is stated to occur at 201.8°C for  $\text{TlBF}_4$  (10) and 266°C for  $\text{TlClO}_4$  (11). In the cases of  $\text{KBF}_4$  (3),  $\text{RbBF}_4$  (4),  $\text{CsBF}_4$  (5) and  $\text{NH}_4\text{BF}_4$  (6) this cubic phase undergoes a further transition at high pressures and temperatures to a modification which was suggested also to be cubic, space group  $Fm\bar{3}m$  (4), with considerably higher disorder. Yet another phase appeared at higher pressures and temperatures in the phase diagrams of  $\text{RbBF}_4$  and  $\text{CsBF}_4$ . Similar phases were expected to appear in the phase diagram of  $\text{TlBF}_4$  (12). Thermal instability prevented the formation of these phases for the perchlorates.

Richter (12) predicted a high-pressure transition for  $\text{TlBF}_4$  similar to that for  $\text{TlClO}_4$  (1).

### Experimental

$\text{TlClO}_4$  was precipitated from aqueous solutions of Merck  $\text{HClO}_4$  and Hopkin and Williams reagent grade  $\text{Tl}_2\text{CO}_3$ , and  $\text{TlBF}_4$  from Hopkin and Williams  $\text{HBF}_4$  and  $\text{Tl}_2\text{CO}_3$ . The salts were dried thoroughly and were characterized by X-ray powder diffraction before use.

Pressures up to 40 kbar were generated in a piston-cylinder apparatus (13, 14). Phase changes were studied by means of differential thermal analysis (D.T.A.) using Chromel-Alumel thermocouples. The samples were enclosed in copper capsules. No reaction was observed between sample and capsule. Heating rates used varied from 0.25–0.5°C/sec. The detailed experimental procedure has been described previously (4, 5). Pressures are believed to be accurate to  $\pm 0.5$  kbar unless otherwise mentioned. Each phase boundary was based on several separate runs. Points plotted are the mean of heating and cooling in the case of solid–solid transitions, but only melting temperatures are plotted in the case of melting curves. Phase changes at high pressures and low temperatures were studied by means of volumetric methods (4, 5).

### Crystallography

The powder pattern of  $\text{TlBF}_4$  II was measured at 207°C, using filtered  $\text{CuK}\alpha$  radiation in a Philips X-86-N high temperature diffractometer attachment. Temperatures were measured by

TABLE I

POWDER PATTERN OF  $\text{TlBF}_4$  II AT  $207^\circ\text{C}$  (FILTERED  $\text{CuK}\alpha$  RADIATION)

$d_{\text{obs}}$ (Å)	$d_{\text{calc}}$ (Å)	$hkl$	I
4.36	4.37	1 1 1	VVS
3.78	3.78	0 0 2	S
2.68	2.68	0 2 2	S
2.28	2.28	1 1 3	VS
2.19	2.18	2 2 2	M
— <sup>a</sup>	1.736	1 3 3	— <sup>a</sup>
1.693	1.692	0 2 4	VW
1.543	1.544	2 4 2	W
1.459	1.456	1 1 5	W
1.337	1.338	0 4 4	VW

<sup>a</sup> Peak obscured by Pt peak from sample holder at same position.

means of a thermocouple welded to the platinum sample support  $\sim 0.2$  cm from the centre of the sample.

The powder pattern of  $\text{TlBF}_4$  II is shown in Table I. All the observed peaks could be assigned on the basis of an fcc unit cell with  $a_0 = 7.566 \pm 0.010$  Å.

$\text{TlBF}_4$  was found to decompose with the evolution of  $\text{BF}_3$  after  $\sim 6$  hours at  $207^\circ\text{C}$ .

## Results

### Thallous Perchlorate

The phase diagram of  $\text{TlClO}_4$  is shown in Fig. 1. The II/I transition yielded strong and sharp signals at atmospheric pressure (Fig. 2 (i)) where the transition temperature was found to be  $267.5^\circ\text{C}$  (mean of four determinations) compared to the literature value of  $266^\circ\text{C}$  (11). On application of pressure the signals became slightly broader, and thermal hysteresis increased from  $\sim 1^\circ\text{C}$  to  $\sim 3^\circ\text{C}$ . This is a consequence of the large volume change (see below) at the transition, which causes a local pressure increase as the transition occurs and thereby broadens the DTA signal. The  $\text{TlClO}_4$  II/III transition line previously studied by Bridgman (1) meets the II/I transition line at the I/III/II triple point at 0.7 kbar,  $280^\circ\text{C}$ . The resulting III/I transition line was followed to 7 kbar,  $410^\circ\text{C}$  where the sample decomposed. A typical signal obtained on this boundary is shown in Fig. 2 (ii). The phase relations of  $\text{TlClO}_4$  are summarized in Table II.

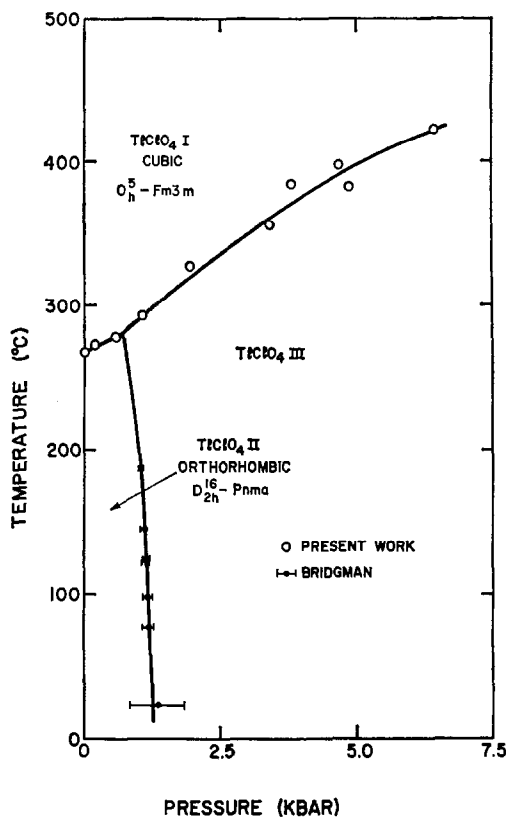


FIG. 1. The phase diagram of  $\text{TlClO}_4$  to 7.5 kbar.

The heat effect associated with the  $\text{TlClO}_4$  II/I transition was measured using a Perkin-Elmer differential scanning calorimeter Model 1B. The transition entropy was found to be

$$\Delta S_{\text{II/I}} = 19.4 \text{ J/deg mole} \approx R \ln 8.$$

The initial slope of the  $\text{TlClO}_4$  II/I phase boundary is  $18^\circ\text{C/kbar}$ , yielding

$$\Delta V_{\text{II/I}} = 3.5 \text{ cm}^3/\text{mole}.$$

Bridgman (1) found that

$$\Delta V_{\text{II/III}} = -1.44 \text{ cm}^3/\text{mole}.$$

The slope of the  $\text{TlClO}_4$  II/III transition line at the III/II/I triple point is  $\sim -250^\circ\text{C/kbar}$ , yielding

$$\Delta S_{\text{II/III}} = 0.6 \text{ J/deg mole} \ll R \ln 2.$$

$\text{TlClO}_4$  II is known to be ordered. The above value of  $\Delta S_{\text{II/III}}$  is too small to be due to disordering, and it follows that  $\text{TlClO}_4$  III must also be ordered. If the usual assumption is made of approximate constancy of transition entropy

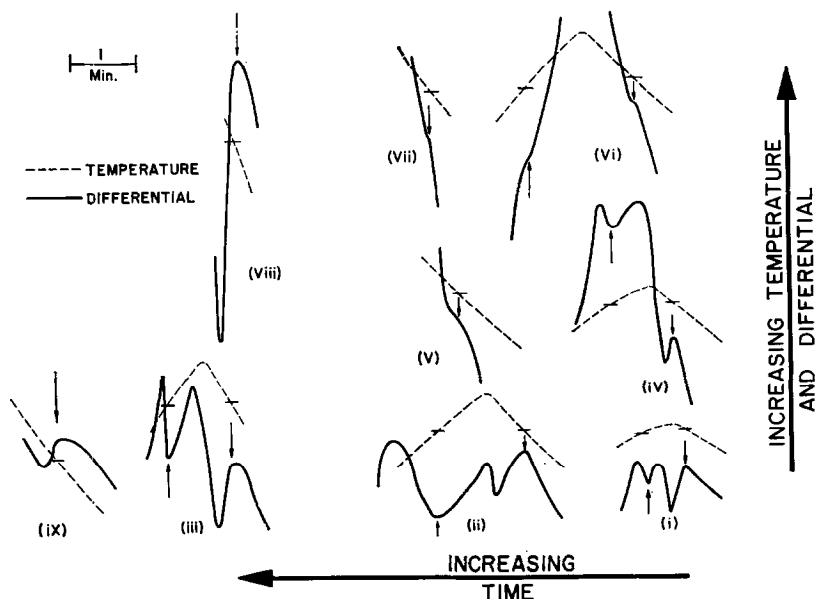


FIG. 2. Typical D.T.A. signals obtained. (i)  $\text{TlClO}_4$  II/I transition at 0 kbar, 267.5°C. (ii)  $\text{TlClO}_4$  III/I transition at 1.1 kbar, 292°C. (iii)  $\text{TlBF}_4$  IV/V transition at 22.7 kbar, 597.7°C. (iv)  $\text{TlBF}_4$  III/II transition at 0 kbar, 201.7°C. (v)  $\text{TlBF}_4$  III/II transition at 5.5 kbar, 360.7°C. (vi)  $\text{TlBF}_4$  II/I transition at 8.8 kbar, 468°C. (vii)  $\text{TlBF}_4$  II/I transition at 7.6 kbar, 473°C. (viii)  $\text{TlBF}_4$  V melting at 17.9 kbar, 670°C. (ix)  $\text{TlBF}_4$  I/V transition at 11.2 kbar, 515°C.

TABLE II  
PHASE RELATIONS OF  $\text{TlBF}_4$  AND  $\text{TlClO}_4$

Transition line	Fit	Standard deviation
$\text{TlClO}_4$ II/I	$t(^{\circ}\text{C}) = 267.5 + 18 P$	1.4°C
$\text{TlClO}_4$ III/I	$t(^{\circ}\text{C}) = 280 + 37 (P - 0.7) - 2.20 (P - 0.7)^2$	7.7°C
$\text{TlClO}_4$ II/III	$P(\text{kbar}) = 0.7 - 0.004 (t - 280) - 0.000007 (t - 280)^2$	0.02 kbar
$\text{TlBF}_4$ III/II	$t(^{\circ}\text{C}) = 201.7 + 36.8 P - 1.597 P^2$	4.8°C
$\text{TlBF}_4$ IV/II	$t(^{\circ}\text{C}) = 350 + 25.9 (P - 5.1) - 1.19 (P - 5.1)^2$	6.0°C
$\text{TlBF}_4$ III/IV	$P(\text{kbar}) = 5.10 - 0.00868 (t - 350) - 0.00001162 (t - 350)^2$	0.02 kbar
$\text{TlBF}_4$ II/I	$t(^{\circ}\text{C}) = 462 + 5.55 P - 0.56 P^2$	2.3°C
$\text{TlBF}_4$ IV/I	$t(^{\circ}\text{C}) = 456.5 + 12.1 (P - 10.6)$	7.7°C
$\text{TlBF}_4$ I/V	$t(^{\circ}\text{C}) = 529 - 1.91 (P - 6.2) - 0.18 (P - 6.2)^2$	0.6°C
$\text{TlBF}_4$ IV/V	$t(^{\circ}\text{C}) = 502 + 11.83 (P - 14.2) - 0.047 (P - 14.2)^2$	3.3°C
$\text{TlBF}_4$ I/liq	$t(^{\circ}\text{C}) = 470 + 16.7 P - 1.10 P^2$	3.2°C
$\text{TlBF}_4$ V/liq	$\frac{P - 6.2}{10.84} = \left(\frac{T}{802}\right)^{4.33} - 1$	3.5°C

Triple point	Pressure (kbar) <sup>a</sup>	Temperature (°C) <sup>a</sup>
$\text{TlClO}_4$ I/III/II	0.7	280
$\text{TlBF}_4$ V/I/liq	6.2	529
$\text{TlBF}_4$ I/V/IV	14.2	502
$\text{TlBF}_4$ I/IV/II	10.6	456.5
$\text{TlBF}_4$ II/IV/III	5.1	350

<sup>a</sup> The accuracies of the triple points can be judged from Figs. 1 and 3.

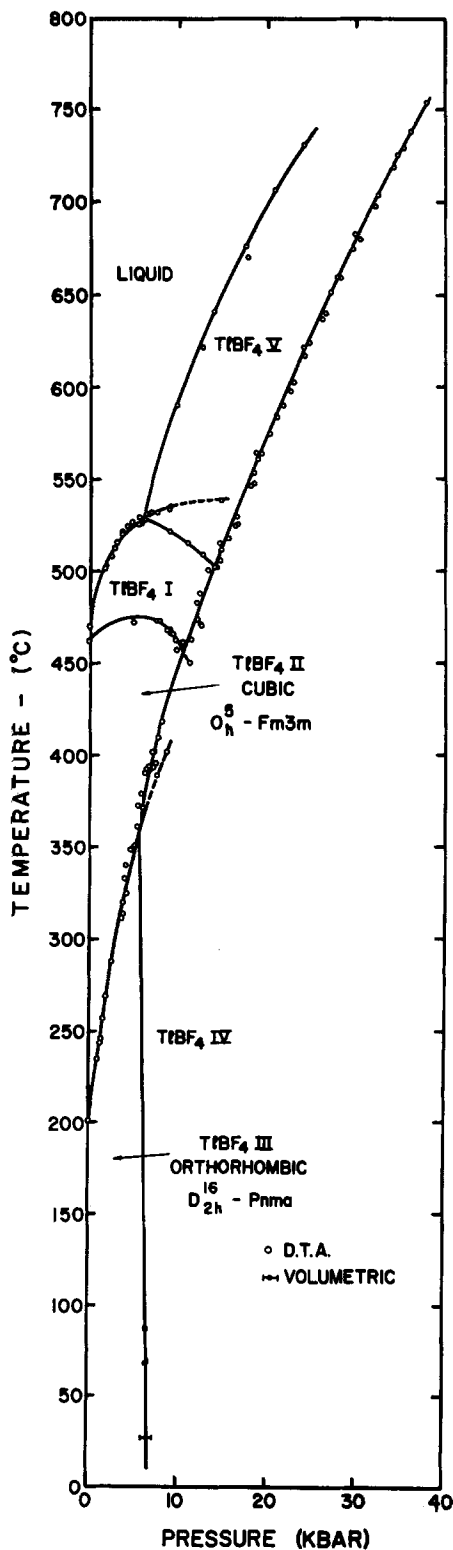


FIG. 3. The phase diagram of  $\text{TlBF}_4$  to 40 kbar.

along the transition lines, the additive relations at the triple point yield

$$\Delta S_{\text{III/I}} = 18.8 \text{ J/deg mole} \approx R \ln 8.$$

The initial slope of the  $\text{TlClO}_4$  III/I transition line is  $37^{\circ}\text{C/kbar}$ , yielding

$$\Delta V_{\text{III/I}} = 7.0 \text{ cm}^3/\text{mole}$$

at the triple point in fair agreement with the value of  $5 \text{ cm}^3/\text{mole}$  to be expected from the additive relations, bearing in mind the experimental uncertainties in the slopes of the  $\text{TlClO}_4$  II/I and III/I transition lines.

#### *Thallos Tetrafluoroborate*

The phase diagram of  $\text{TlBF}_4$  is shown in Fig. 3. The expected counterpart of the  $\text{TlClO}_4$  II/III transition was found at  $6.73 \pm 0.60$  kbar at  $26.6^{\circ}\text{C}$  by means of piston rotation. It was also encountered at  $67.9^{\circ}\text{C}$ ,  $6.606 \pm 0.161$  kbar and at  $86.6^{\circ}\text{C}$ ,  $6.575 \pm 0.130$  kbar. The volume change was  $1.5 \text{ cm}^3/\text{mole}$ . A typical curve of piston load versus piston displacement is shown in Fig. 4.

The  $\text{TlBF}_4$  III/II transition yielded sharp clear signals at atmospheric pressure (Fig. 2 (iv)). The  $\sim 10^{\circ}\text{C}$  thermal hysteresis was essentially independent of heating/cooling rate in the range  $0.25$ – $1.5^{\circ}\text{C/sec}$ , but decreased slightly at lower heating/cooling rates (Fig. 5). The pre-

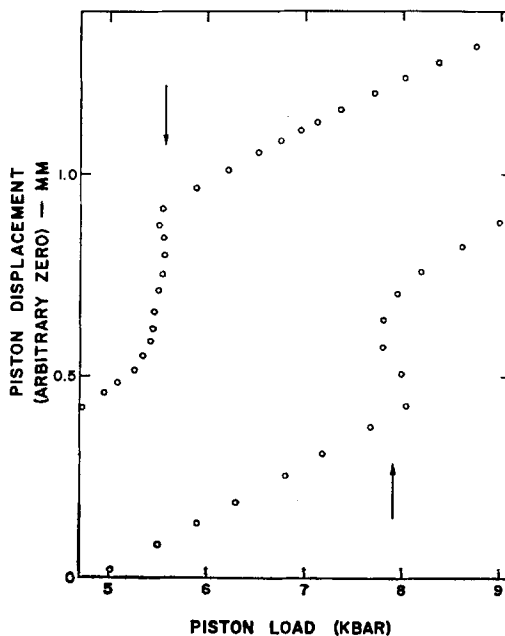


FIG. 4. Curve of piston displacement versus piston load for  $\text{TlBF}_4$ , showing the new III/IV transition.

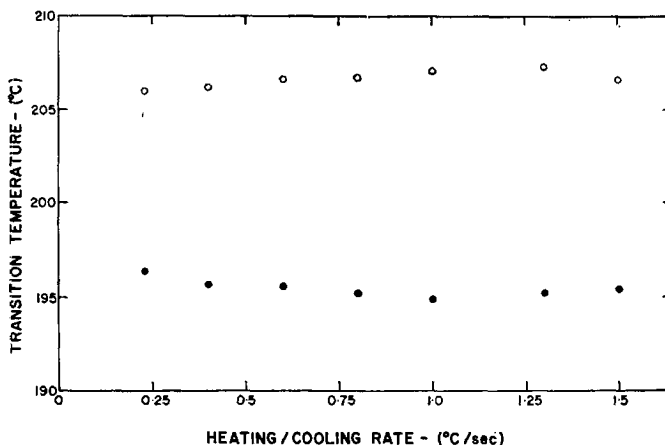


FIG. 5. Dependence of the  $\text{TlBF}_4$  III/II transition temperature at atmospheric pressure on the rate of heating and cooling. Open circles, heating; closed circles, cooling.

sent atmospheric pressure transition point is  $201.7^\circ\text{C}$  (mean of twelve determinations) in excellent agreement with the earlier value of  $201.8^\circ\text{C}$  (10). At higher pressures the DTA signals corresponding to the III/II transition broadened considerably (Fig. 2 (v)) due to the large volume change upon transition (see below). The  $\text{TlBF}_4$  III/II transition line is terminated at the  $\text{TlBF}_4$  II/IV/III triple point at 5.1 kbar,  $350^\circ\text{C}$ . The III/IV transition near this triple point evidently is either slow or has a large region of indifference as the metastable extension of the III/II boundary could be followed  $\sim 3$  kbar beyond the triple point. The resulting  $\text{TlBF}_4$  IV/II boundary rises steeply with pressure. Thermal hysteresis on the IV/II boundary ranged from  $2$ – $6^\circ\text{C}$ . The  $\text{TlBF}_4$  IV/II transition line is terminated at the I/IV/II triple point at 10.6 kbar,  $456.5^\circ\text{C}$  with the appearance of a new phase  $\text{TlBF}_4$  I. The  $\text{TlBF}_4$  II/I transition signals became smaller with decreasing pressure (Fig. 2 (vi) and (vii)), as was the case for the corresponding  $\text{CsBF}_4$  II/I (5) and  $\text{RbBF}_4$  I/IV (4) transitions. Nevertheless, it was possible to obtain a point on this transition line at atmospheric pressure, where the transition temperature was  $462^\circ\text{C}$ . It is clear that the II/I transition line passes through a maximum at 5 kbar,  $476^\circ\text{C}$ .

The  $\text{TlBF}_4$  IV/I transition line rises with pressure, and yields DTA signals similar to those shown in Fig. 2 (iii). The slope change at the  $\text{TlBF}_4$  V/IV/I triple point at 14.2 kbar,  $502^\circ\text{C}$  is small, viz., from 12.1 to  $11.8^\circ\text{C/kbar}$ . The resulting  $\text{TlBF}_4$  IV/V transition yields strong DTA signals (Fig. 2 (iii)) similar to those for the

IV/I transition, with thermal hysteresis ranging from  $0$ – $4^\circ\text{C}$ . No further new phases were encountered to 40 kbar. The  $\text{TlBF}_4$  I/V transition yielded clear but somewhat broad DTA signals (Fig. 2 (ix)) with less than  $\sim 2^\circ\text{C}$  thermal hysteresis.

The melting point of  $\text{TlBF}_4$  I at atmospheric pressure was determined in three separate experiments, and found to be  $470 \pm 3^\circ\text{C}$ . The as yet unsealed capsules invariably leaked immediately after melting at atmospheric pressure. However, a large number of points on the melting curve of  $\text{TlBF}_4$  I were obtained in other runs after sealing the capsules *in situ*. The  $\text{TlBF}_4$  V/I/liquid triple point at 6.2 kbar,  $529^\circ\text{C}$  is marked by a sharp inflection in the melting curve. However, the metastable extension of the melting curve of  $\text{TlBF}_4$  I could be followed to considerably beyond the triple point on increase of pressure. The melting curve of  $\text{TlBF}_4$  V rises very steeply with pressure. A typical DTA signal on this line is shown in Fig. 2 (viii). The melting curve of  $\text{TlBF}_4$  V was followed only to  $730^\circ\text{C}$ , 24 kbar. Severe leakage problems, possibly due to the large volume change upon melting (note the steepness of the melting curve), were consistently encountered and prevented satisfactory corrections for friction. This melting curve can be considered correct only to  $\pm 1$  kbar.

The phase relations of  $\text{TlBF}_4$  are summarized in Table II. The melting curves were fitted to the Simon equation (15)

$$P - P_0 = A \left[ \left[ \frac{T}{T_0} \right]^c - 1 \right]$$

where  $T^{\circ}K$  is the melting point at  $P$  kbar,  $P_0$  and  $T_0$  the coordinates of the triple point of the phase in question, and  $A$  and  $c$  are adjustable constants, determined by means of Babb's method (16).

The entropy of the  $\text{TlBF}_4$  III/II transition, as determined by means of a differential scanning calorimeter, is

$$\Delta S_{\text{III/II}} = 18.9 \text{ J/deg mole} \simeq R \ln 8$$

closely similar to the value for the  $\text{TlClO}_4$  II/I transition. The initial slope of the  $\text{TlBF}_4$  III/II transition line is  $36.8^{\circ}\text{C/kbar}$  and the slope at the IV/III/II triple point is  $20.2^{\circ}\text{C/kbar}$ , yielding, on the assumption that  $\Delta S_{\text{III/II}}$  remains approximately constant along the transition line,

$$(\Delta V_{\text{III/II}})_{P=0} = 6.9 \text{ cm}^3/\text{mole}$$

and

$$(\Delta V_{\text{III/II}})_{P=5.1} = 3.8 \text{ cm}^3/\text{mole}.$$

The slope of the  $\text{TlBF}_4$  III/IV transition line is  $\sim -330^{\circ}\text{C/kbar}$  in the temperature region  $20$ – $80^{\circ}\text{C}$ , and in this region

$$\Delta V_{\text{III/IV}} = -1.5 \text{ cm}^3/\text{mole} \text{ (see above),}$$

yielding

$$\Delta S_{\text{III/IV}} = 0.5 \text{ J/deg mole} \ll R \ln 2$$

closely similar to the value obtained for the  $\text{TlClO}_4$  II/III transition. At the triple point the volume change can be expected to be somewhat less in view of the curvature of the phase boundary. The additive relations at the triple point then yield

$$\Delta S_{\text{IV/II}} = 18.4 \text{ J/deg mole}$$

and

$$\Delta V_{\text{IV/II}} \simeq 5 \text{ cm}^3/\text{mole}$$

with an initial slope of  $\sim 26^{\circ}\text{C/kbar}$  in excellent agreement with the value of  $25.8^{\circ}\text{C/kbar}$  directly observed.

Attempts were made to measure the latent heat of the  $\text{TlBF}_4$  II/I transition at atmospheric pressure, but decomposition or sublimation of the uncontained sample was evident even at somewhat lower temperatures.

## Discussion

As has been the case in previous studies in this series (2–6), the phase diagrams of  $\text{TlClO}_4$  and  $\text{TlBF}_4$  are strikingly similar. In particular, the slopes of the  $\text{TlClO}_4$  II/I and  $\text{TlBF}_4$  III/II transition lines at the  $\text{TlClO}_4$  III/II/I and

$\text{TlBF}_4$  IV/III/II triple points are 18 and  $20.2^{\circ}\text{C/kbar}$ , respectively, and the entropies of these two transitions are nearly identical. Similarly, the initial volume changes of the  $\text{TlClO}_4$  III/I and  $\text{TlBF}_4$  IV/II transitions are closely the same ( $\sim 5 \text{ cm}^3/\text{mole}$ ). The entropies and volume changes of the  $\text{TlClO}_4$  II/III and  $\text{TlBF}_4$  III/IV transitions are of the same magnitude. If decomposition of  $\text{TlClO}_4$  at higher temperatures could have been prevented, the phase diagram of  $\text{TlClO}_4$  at higher temperatures could be expected to be quite similar to that of  $\text{TlBF}_4$ .

The ionic radius of  $\text{Tl}^+$  is intermediate between those of  $\text{Rb}^+$  and  $\text{Cs}^+$ , but much closer to that of  $\text{Rb}^+$  (17). However, the large polarizability of the  $\text{Tl}^+$  ion is known to cause some deviations from ideal ionic behaviour, e.g., in the case of the thallos halides (18). In the present case the phase diagram of  $\text{TlBF}_4$  is intermediate between those of  $\text{RbBF}_4$  (4) and  $\text{CsBF}_4$  (5), and no phases, at least at or above room temperature, were found for which counterparts were not available in the phase diagram of  $\text{RbBF}_4$ . In fact, it would appear probable that  $\text{RbBF}_4$  II and  $\text{TlBF}_4$  III,  $\text{RbBF}_4$  III and  $\text{TlBF}_4$  IV,  $\text{RbBF}_4$  I and  $\text{TlBF}_4$  II,  $\text{RbBF}_4$  IV and  $\text{TlBF}_4$  I, and finally,  $\text{RbBF}_4$  V and  $\text{TlBF}_4$  V are isostructural pairs.

It has been previously suggested that the family of phases  $\text{KBF}_4$  III,  $\text{RbBF}_4$  IV,  $\text{CsClO}_4$  I and  $\text{CsBF}_4$  I, to which must now be added  $\text{TlBF}_4$  I, is cubic with the same space group, but higher disorder, as the family  $\text{KBF}_4$  I,  $\text{RbBF}_4$  I,  $\text{CsClO}_4$  II and  $\text{CsBF}_4$  II, to which must now be added  $\text{TlBF}_4$  II. While this suggestion cannot be ruled out, an argument against it is the consistent observation that, e.g., the  $\text{TlBF}_4$  II/I transition becomes increasingly more difficult to observe at lower pressures. The  $\text{CsBF}_4$  II/I transition could not be definitely observed below  $\sim 6$  kbar, although a possible but doubtful point at atmospheric pressure was measured. This may indicate that a considerable structural difference exists between the two families of phases. A high-temperature X-ray diffraction study of, for instance,  $\text{CsBF}_4$  I would be extremely informative, if means could be devised to prevent decomposition.

## Acknowledgments

The authors would like to thank Martha C. Pistorius for writing the computer programs used in fitting the data, and Dr. P. W. Richter for valuable discussions. J. Erasmus

and his staff and A. de Kleijn and his staff kept the equipment in good repair, and were responsible for the manufacture of the furnace parts. Calculations were carried out on the IBM System 360/65 H of the National Research Institute for Mathematical Sciences. The DSC studies were carried out by S. Pretorius of the S. A. Coal, Oil and Gas Corporation, Limited.

## References

1. P. W. BRIDGMAN, *Proc. Amer. Acad. Arts Sci.* **72**, 45 (1937).
2. C. W. F. T. PISTORIUS, J. C. A. BOEYENS, AND J. B. CLARK, *High Temp. High Press.* **1**, 41 (1969).
3. C. W. F. T. PISTORIUS, *J. Phys. Chem. Solids* **31**, 385 (1970).
4. C. W. F. T. PISTORIUS AND J. B. CLARK, *High Temp. High Press.* **1**, 561 (1969).
5. P. W. RICHTER AND C. W. F. T. PISTORIUS, *J. Solid State Chem.* **3**, 197 (1971).
6. P. W. RICHTER AND C. W. F. T. PISTORIUS, *J. Solid State Chem.* **3**, 434 (1971).
7. W. BÜSSEM AND K. HERRMANN, *Z. Krist.* **67**, 405 (1928).
8. C. W. F. T. PISTORIUS, *Z. Anorg. Allg. Chem.* **376**, 308 (1970).
9. R. W. G. WYCKOFF, "Crystal Structures," Vol. 3, pp. 45-58, Interscience, New York, 1965.
10. O. HASSEL AND J. A. HVEDING, *Arch. Math. Naturvidenskab* **45**, 2, 33 (1941).
11. B. KANELLAKOPOULOS, *J. Inorg. Nucl. Chem.* **28**, 813 (1966).
12. P. W. RICHTER, Ph.D. dissertation, University of South Africa, December 1971.
13. G. C. KENNEDY AND R. C. NEWTON, in "Solids under Pressure" (W. PAUL AND D. M. WARSCHAUER, Eds.), McGraw-Hill, New York, 1963.
14. G. C. KENNEDY AND P. N. LA MORI, in "Progress in Very High Pressure Research" (F. P. BUNDY, W. R. HIBBARD, AND H. M. STRONG, Eds.), p. 304, Wiley, New York, 1961.
15. F. E. SIMON AND G. GLATZEL, *Z. Anorg. Allg. Chem.* **78**, 309 (1929).
16. S. E. BABB, *Rev. Mod. Phys.* **35**, 400 (1963).
17. R. D. SHANNON AND C. T. PREWITT, *Acta Cryst.* **B25**, 925 (1969).
18. C. W. F. T. PISTORIUS AND J. B. CLARK, *Phys. Rev.* **173**, 692 (1968).